2
Shape dependence of FIF

2.1 Dimensional considerations

Let us consider two microscopic neutral objects (say atoms or molecules) of characteristic sizes a_1 and a_2 in three dimensions at separations $r \gg a_1, a_2$. Due to overall charge neutrality of the objects, typical charge fluctuations generate dipoles, quadrapoles, and higher multipoles. At large separations the dipolar fluctuations are most relevant, with direct interactions proportional to the product of polarizabilities, which scales as $a_1^3 a_2^3$. From this information, as well as an energy scale, we can build up the form of long-range FIF (up to a numerical coefficient) from dimensional analysis.

There are in fact three regimes:

Thermal fluctuations provide an energy scale of $k_B T$, suggesting an interaction potential of the form

$$U_T(r) \sim k_B T \frac{a_1^3 a_2^3}{r^6}. \tag{2.1}$$

This behavior is expected to hold for separations $r > \lambda_T = \frac{\hbar c}{k_B T}$. At room temperature, with $\lambda_T \sim 8\mu$m, interactions at such large scales are too weak to be of relevance to molecules.

Quantum fluctuations are more important than thermal ones for $r < \lambda_T$, suggesting interactions of the form

$$U_Q(r) \sim \hbar c \frac{a_1^3 a_2^3}{r^7}. \tag{2.2}$$

This regime is usually referred to as the *retarded van der Waals* interactions.

Non-retarded van der Waals interactions correspond to sufficiently short scales, where the spacing to the first excited state of the atom, $\hbar\omega_0$, sets the relevant energy scale, leading to

$$U_{vdW}(r) \sim \hbar\omega_0 \frac{a_1^3 a_2^3}{r^7}. \tag{2.3}$$

The transition to the retarded regime occurs for $r > c/\omega_0$, roughly around 20nm for hydrogen.

The next important geometry concerns interaction of a compact object of size a with a plate. The fluctuation-induced interaction at large separations $H \gg a$ is expected to be dominated by dipole fluctuations, and hence proportional to the polarizability $\chi \propto a^3$. Dimensional analysis then suggests FIF of the forms

$$F_T \sim k_B T \frac{a^3}{H^4} \qquad \text{(thermal)}, \tag{2.4}$$

$$F_Q \sim \hbar c \frac{a^3}{H^5} \qquad \text{(retarded van der Waals)}, \tag{2.5}$$

$$F_{vdW} \sim \hbar \omega_0 \frac{a^3}{H^4} \qquad \text{(van der Waals)}, \tag{2.6}$$

in the corresponding regimes. However, as the compact object approaches the surface its shape and internal structure become more relevant; higher order multiploes and their interactions with the surface resulting in more complex FIF.

Since FIF are inherently many-body interactions computing the exact form of the interaction is a difficult task and various approximation schemes have been developed. One scheme is based on pairwise summation of van der Waals forces between different volume elements; the resulting sums are typically proportional to the volume of a compact body. Another scheme is based on the Casimir force between parallel plates, obtaining the net interaction for objects in close proximity as if arising from summation of contributions from surface elements facing each other. This proximity force approximation (PFA) is indeed asymptotically exact, and in fact widely used in interpretation of Casimir force experiments where a large sphere approaches a surface. However, only recently systematic corrections to PFA (in terms of surface curvatures) have been computed.

As illustration of importance of shape, consider the quantum Casimir interaction of a perfectly conducting cylinder of radius R and length L at a separation H from a mirror, with $R \ll H \ll L$. We expect the interaction to be of a form than vanishes as $R \to 0$, but how? Pair-wise summation leads to a force proportional to the volume $R^2 L$, suggesting

$$U_{pairwise} \sim \hbar c \frac{LR^2}{H^4}. \tag{2.7}$$

Approximating the cylinder with a ribbon suggests an area of LR presented parallel to the mirror, and hence a Casimir interaction of

$$U_{ribbon} \sim \hbar c \frac{LR}{H^3}. \tag{2.8}$$

The proximity force approximation, which more systematically adds small ribbon elements at varying separations leads to

$$U_{PFA} \sim \hbar c \frac{LR^{1/2}}{(H-R)^{5/2}}. \tag{2.9}$$

The correct result in the limit of $R \to 0$ is

$$U_{exact} \sim \hbar c \frac{L}{H^2 \ln(H/R)}, \tag{2.10}$$

due to dominant long-wavelength current fluctuations along the wire.

2.2 Scale invariant shapes

One difficulty with computations for compact objects, even when idealized as perfect conductors (hence presenting no additional energy scales from resonances) is the

presence of multiple length scales (e.g. due to typical extent R). This difficulty is alleviated for a class of objects that are scale invariant, presenting no characteristic intrinsic length scale. Examples include the plane, cone, pyramid, and wedge, all of infinite extent. These objects can still be characterized by dimensionless angles (such as the opening of the cone, or of the wedge), but no length. If two such objects are brought to proximity, the combined system presents only a single length scale, e.g from the nearest distance from the apex of a cone to a plane, which we designate as H. Forces between the two objects can now be obtained (up to a numerical constant) by dimensional analysis.

The simplest case corresponds to two parallel plates at separation H. In the case the relevant force needs to be proportional to area, and the corresponding pressures will have the forms k_BT/H^3 and $\hbar c/H^4$ as obtained previously. For two wedges (or a wedge and plane) held parallel, the forces must be proportional to wedge length, and force per unite length must scale as k_BT/H^2 and $\hbar c/H^3$. The overall amplitude will now depend on the opening angle of the wedge. Finally, when a cone is brought to proximity with a plane, we expect forces of the form k_BT/H and $\hbar c/H^2$, with amplitudes that reflect opening angle of the cone, and its orientation to the plane. Computation of these (still universal) amplitudes is still difficult, but possible in certain cases, as will be shown next in connection with polymers.

2.3 Entropic force from polymers

The flexibility of a long polymer arises from the statistical fluctuations of segments larger than the persistence length. The important parameter that governs the number of configurations is thus not the degree of polymerization N, but the number of unconstrained degrees of freedom, or the *Kuhn* length $N_K \approx Na/(2\xi_p)$. To see this explicitly, let us consider the *end to end separation* of the polymer, given by

$$\vec{R} = \vec{t}_1 + \vec{t}_2 + \cdots + \vec{t}_N = \sum_{i=1}^{N} \vec{t}_i \, .$$

Because of rotational symmetry (there is no cost for rotating the entire polymer), $\langle \vec{R} \rangle = 0$, and its variance is given by

$$\langle R^2 \rangle = \sum_{i,j=1}^{N} \langle \vec{t}_i \cdot \vec{t}_j \rangle = Na^2 + 2 \sum_{i<j} \langle \vec{t}_i \cdot \vec{t}_j \rangle \, . \tag{2.11}$$

We shall assume that the orientational correlations decay as a simple exponential (this is only asymptotically correct), i.e.

$$\langle \vec{t}_i \cdot \vec{t}_j \rangle = a^2 e^{-a|i-j|/\xi_p} \, . \tag{2.12}$$

As the correlation function is the same for every pair of points separated by a distance k, and as there are $(N-k)$ such pairs along the chain

$$\langle R^2 \rangle = Na^2 + 2a^2 \sum_{k=1}^{N} (N-k) e^{-ak/\xi_p} \, . \tag{2.13}$$

The above geometric series are easily summed, and for $N \gg 1$ (where only the term proportional to N is significant), we obtain

$$\langle R^2 \rangle = Na^2 \left(1 + \frac{2e^{-a/\xi_p}}{1 - e^{-a/\xi_p}} \right) = Na^2 \coth \left(\frac{a}{2\xi_p} \right) \tag{2.14}$$

$$\approx 2Na\xi_p = (2\xi_p)^2 \left(\frac{Na}{2\xi_p} \right) . \tag{2.15}$$

The approximations in the second line rely on $\xi_p \gg a$. The very last expression indicates that the behavior of the variance is the same as that of $N_K \equiv (Na/2\xi_p)$ independent segments of length $2\xi_p$, i.e. the same variance is obtained for a collection of N_K *freely–jointed rods*, each of length $2\xi_p$. Indeed the correlations between these Kuhn segments is sufficiently small that in the limit of $N_K \gg 1$, we expect the *Central Limit Theorem* to hold, leading to the probability distribution function

$$p(\vec{R}\,) = \exp \left[-\frac{3R^2}{2\langle R^2 \rangle} \right] \left(\frac{2\pi \langle R^2 \rangle}{3} \right)^{3/2} = \exp \left[-\frac{3R^2}{4Na\xi_p} \right] \frac{1}{(4\pi Na\xi_p/3)^{3/2}} . \tag{2.16}$$

The final probability distribution is identical to the Boltzmann weight of a Hookian spring of strength $J_{polymer}$ connecting the end points of the polymer, and the result of entropic fluctuations can be interpreted as conferring an elastic bond between the ends of the polymer with spring coefficient

$$J_{polymer} = \frac{3k_BT}{\langle R^2 \rangle} = \frac{3k_BT}{2Na\xi_p}. \tag{2.17}$$

For future reference, note that for real polymers, self-avoidance and other (short-range) interactions modify the scale form to

$$\langle R^2 \rangle \simeq a^2 N^{2\nu} \tag{2.18}$$

with $\nu \approx 0.59$ in three dimensions.

2.3.1 Force between plates

The overall partition function of a random walk, without constraints is expected to scale as c^N, with c encoding (non-universal) contributions to energy and entropy. When constrained to have end points separated by $\mathbf{x}$, it takes the functional form

$$Z(N, \mathbf{x}) = \frac{c^N}{(2\pi Na^2)^{3/2}} \exp \left(-\frac{x^2}{2Na^2} \right) . \tag{2.19}$$

Note that the part of Z relevant to discussions of FIF satisfies the diffusion equation

$$\frac{\partial Z}{\partial N} = a^2 \nabla^2 Z \, , \tag{2.20}$$

and this form can be used to tackle other forms of constraints. For example, consider the Casimir-like setup in which a very long polymer is confined between two solid plates.

With the boundary conditions, $Z(0) = Z(H) = 0$, the appropriate asymptotic solution is $Z(z) \propto \sin(\pi z/H)$. With a corresponding eigenvalue of $\lambda_0 = -a^2\pi^2/H^2$, this leads to

$$Z(N,H) \propto \exp\left(-\frac{Na^2\pi^2}{H^2}\right). \tag{2.21}$$

The reduction in entropy, then leads to a repulsive entropic force of

$$F(H) = k_B T \frac{\partial \ln Z(N,H)}{\partial H} = k_B T \frac{Na^2\pi^2}{H^3} = k_B T \frac{\pi^2}{3}\frac{\langle R^2\rangle}{H^3}. \tag{2.22}$$

2.3.2 Depletion near a surface

The dependence $Z(z) \propto \sin(\pi z/H)$ indicate that the probability to find the polymer end point near a rigid surface (close to $z = 0$ or $z = H$) goes to zero linearly. This can also be seen by using the method of images to find the solution to the diffusion equation with the single boundary condition $Z(z) = 0$. It is easy to check that

$$Z_S(N,x) = a\frac{d}{dz}\frac{1}{(2\pi Na^2)^{3/2}}\exp\left(-\frac{x^2}{2Na^2}\right) = \frac{az}{Na^2(2\pi Na^2)^{1/2}}\exp\left(-\frac{x^2}{2Na^2}\right), \tag{2.23}$$

is such a solution, vanishing linearly as $z \to 0$.

Integrating over all positions of the end point yields

$$Z_S(N) = \int d^3\mathbf{x} Z_S(N,x) = a\int_0^\infty dz \frac{d}{dz}\frac{1}{(2\pi Na^2)^{1/2}}\exp\left(-\frac{z^2}{2Na^2}\right) = \frac{1}{\sqrt{2\pi N}}, \tag{2.24}$$

i.e. a reduction in the partition function of a random walk starting close to the surface by a factor of $\sqrt{N}$. Quite generally, the partition function of a polymer depends on its length as $Z(N) \simeq c^N N^{\gamma-1}$. The universal exponent γ depends on general properties of the polymer (e.g. ideal or self-avoiding), as well as constraints (such as its topology, or constraints). Clearly $\gamma = 1$ for an unconstrained random walk in space, while the above calculation indicates $\gamma_S = 1/2$ for a random walk starting close to an impenetrable surface.

In the following we shall explore behavior of polymers with one end-point close to a scale invariant obstacle. In the vicinity of the obstacle the end-point probability vanishes as z^p (generalizing from the linear reduction near a plane). Integrating such dependence (up to a characteristic separation $z \sim N^\nu$) then leads to $Z(N) \simeq c^N N^{\gamma-1}$ with the exponent identity

$$\gamma - 1 = -p\nu, \tag{2.25}$$

which we shall exploit shortly.

2.3.3 Force on a conical tip

Consider an idealized setup in which a polymer is attached to the tip of a solid cone, approaching a solid plate (or another cone). This exemplifies a geometry of obstacles in which the only (non-microscopic) length scale is provided by the tip-plate (or tip-tip) separation h. The polymer itself undergoes self-similar fluctuations, spanning length

scales intermediate between microscopic (monomer size, or persistence length a) and macroscopic. The latter is set by the typical end-to-end distance R_0, or by the radius of gyration R_g (which differs from R_0 only by a multiplicative factor of order of unity). The typical size of the polymer grows with the number of monomers N through the scaling relation $R_0 \sim R_g \propto N^\nu$. The self-similar shape of the obstacles also presumably extends only up to a characteristic scale H, say the height beyond which the cone is terminated or changes shape.

Neglecting any structure (and hence energy) associated with the polymer, variations in free energy as the cone (plus tip-attached polymer) approaches the plate are entirely entropic in origin and proportional to k_BT. The entropic force has dimensions of energy divided by length, and at separations $a \ll h \ll R_0 \ll H$ the relevant length scale is h, and it is reasonable to posit

$$F = \mathcal{A}\,\frac{k_BT}{h}\ . \tag{2.26}$$

This is because the polymer configurations are constrained only on the scale of confinement h; increasing the length of the polymer or the size of the cone (as long as $h \ll R_0 \ll H$) should not influence the force; furthermore the entropy change is independent of a.

Indeed, the simple force law of Eq. (**??**) applies to all circumstances where the separation provides the only relevant length scale. The dimensionless amplitude $\mathcal{A}$ will depend on geometric factors characterizing the confining boundaries such as the opening angle of a cone Θ (and if tilted, on the corresponding angle). It will also depend on factors that characterize the scaling of polymeric fluctuations, thus differing in cases of ideal and self-avoiding polymers, and for linear, star, and brush polymers. In the following we shall demonstrate that in a number of setups, the amplitude $\mathcal{A}$ can be related to variations of the (universal, but shape dependent) exponent p, characterizing polymeric depletion near an obstacle.

A random walk starting at the tip of a cone provides a first approximation to a polymer linked to the tip of an AFM probe as depicted in Fig. **??**a. With the cone far away from a plate ($h \gg R_g$), the number of configurations of the polymer grows with the number of monomers as

$$\mathcal{N}_{\rm c} = b\, z^N N^{\gamma_{\rm c}(\Theta)-1}, \tag{2.27}$$

where the effective coordination number z, as well as the pre-factor b, depend on the microscopic details (such as the scale a), while the 'universal' exponent $\gamma_{\rm c}$ only depends on the cone angle. When the cone touches the plate as in Fig. **??**c, the number of configurations is reduced to $\mathcal{N}_{\rm cp}$ with exponent $\gamma_{\rm cp}(\Theta)$. We shall henceforth use an exponent subscript 's' (as in $\gamma_{\rm s}$) to refer to the above cases, with "s=c" for cone and "s=cp" for cone+plate; the absence of a subscript (as in γ) will signify a free polymer. The work done against the entropic force in bringing in the tip from afar to contact the plate can now be computed as

$$W = \int_a^{R_0} {\rm d}h\ \mathcal{A}\frac{k_BT}{h}\ = \mathcal{A}k_BT\ln\frac{R_0}{a} = \mathcal{A}\,\nu k_BT\ln N. \tag{2.28}$$

This work can also be computed from the change in free energies between the final and initial states, due to the change in entropy, as

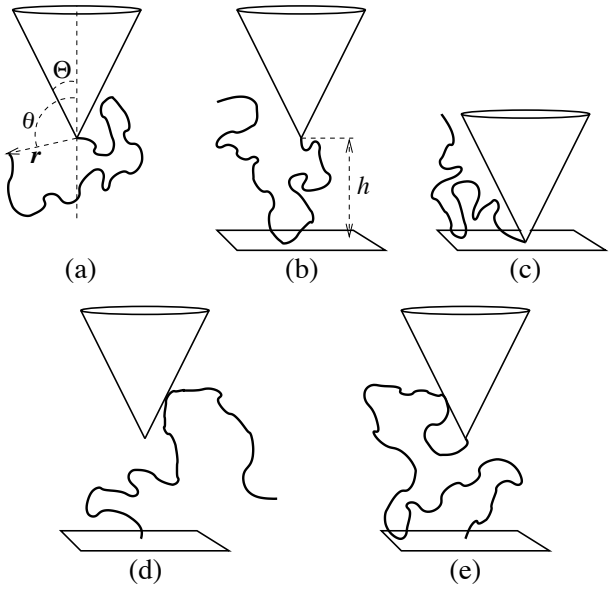

Fig. 2.1 (a) Polymer attached to the tip of a solid cone with apex semi-angle Θ (configuration "c"); positions are described by the spherical coordinates r, θ and azimuthal angle ϕ (not shown). (b) The tip, where the polymer is attached, is at a distance $h \ll R_0$ from the plate. (c) The tip touching the plate (configuration "cp"). (d) Tip is at a finite distance from a plate to which the polymer is attached. (e) Polymer attached to both surfaces.

$$\Delta\mathcal{F} = -T\Delta\mathcal{S} = T\mathcal{S}_{\rm c} - T\mathcal{S}_{\rm cp} = k_B T(\gamma_{\rm c} - \gamma_{\rm cp}) \ln N \,, \tag{2.29}$$

with the entropy $\mathcal{S} = -k_B \ln \mathcal{N}$ computed from Eq. (**??**). By equating W and $\Delta\mathcal{F}$ we find

$$\mathcal{A} = \frac{\gamma_{\rm c} - \gamma_{\rm cp}}{\nu} = p_{\rm cp} - p_{\rm c} \,; \tag{2.30}$$

the final result obtained from the scaling law $\gamma - 1 = -p\nu$.

The arguments presented in the previous paragraph rely only on the fact that configurations of the obstacles lack a length scale for both $h \to 0$ and $h \to \infty$. Consequently, similar reasoning can be applied to a variety of objects such as those depicted in Fig. **??**, or combinations of such objects. The force prefactor is then related to the exponents in the initial and the final states by

$$\mathcal{A} = \frac{\gamma^{\rm initial} - \gamma^{\rm final}}{\nu} = p^{\rm final} - p^{\rm initial} \,. \tag{2.31}$$

Consider, for instance, an ideal polymer in free space (or held by a point-like object (Fig. **??**g)). Its number of configurations is z^N, i.e. $\gamma \equiv \gamma_0 = 1$, and correspondingly $\eta_0 = 0$. If the end of the polymer is brought into contact with a plane, then in any space dimension d the number of configurations scales as $z^N N^{-1/2}$, i.e. with $\gamma \equiv \gamma_{\rm p0} = 1/2$, and corresponding to $\eta_{\rm p0} = 1$. Thus for a long polymer held by a point-like object at a

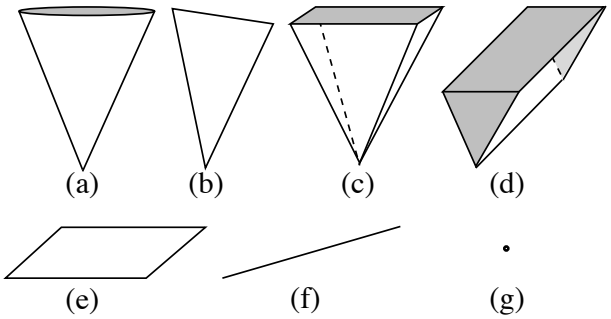

Fig. 2.2 Examples of three dimensional figures without a length scale; grey surfaces indicate truncation only for graphical representations. (a) circular cone, (b) two-dimensional sector of a circle (in 3D space), (c) pyramid, (d) wedge, (e) plane, (f) line, (g) point. A polymer is to be attached to the point (g), to the apex of (a), (b), (c); or to any point on the edge of (d), or the entirety of (e) or (f). The plane and line can also be semi-infinite with a polymer attached to their edge or end-point.

distance h from a plane, the entropic force has a prefactor $\mathcal{A} = 1$. This result is valid for any d.

When the obstacles are separated by h, the loss of polymer entropy (and the corresponding pressure leading to a force concentrated in the confinement region. The part of the polymer that wanders away from this area is relatively unperturbed and does not contribute to the force, which for large N is independent of polymer size. This is not the case when the entire polymer contributes to the force, as for a polymer held between two plates, where the force is proportional to N. Thus, the argument fails when dimensionality of the system is changed between the initial and final states. For example when a 3-dimensional polymer connected to a two-dimensional plane approaches a parallel plane, in the final configuration the confined polymer is essentially two-dimensional. Free energies in the initial and final state have different extensive parts, and the polymer-mediated force depends on the number of monomers.

It is worth reiterating that by focusing on entropy, we have assumed that the only interaction between the polymer and the obstacles is due to hard-core exclusion. Attractive interactions between the polymer and surface will introduce temperature dependent corrections, and additional size scales. Weak interactions are asymptotically irrelevant, but strong interactions may lead to a phase in which the polymer is absorbed onto the obstacles, rendering the entropic considerations presented here inappropriate. Real obstacles are self-similar over a range of length scales; for example an AFM tip may be rounded, or abruptly change its angle.

2.3.4 Two dimensional wedge

Behavior of a random walk near an obstacle can be explored by study of solutions of the Laplace equation with appropriate boundary conditions. For an object with the symmetry of a cone (generalized to d spatial dimensions), the solutions can be cast in the form $Z(r, \theta) = r^p \Psi(\theta)$ in terms of a radial coordinate r, and the polar angle θ. Substituting the above form (dictated by symmetry) in the generalized Laplace

equation, we find that the exponent p satisfies

$$\frac{1}{(\sin\theta)^{d-2}}\frac{d}{d\theta}\left[(\sin\theta)^{d-2}\frac{d\Psi}{d\theta}\right]+p(d-2+p)\Psi(\theta)=0\,, \tag{2.32}$$

subject to the appropriate boundary conditions. For an isolated cone, the function $\Psi_{\rm c}$ must be positive and regular outside the cone, with $d\Psi_{\rm c}/d\theta|_{\theta=\pi}=0$ to avoid a cusp on the symmetry axis, and $\Psi_c(\Theta)=0$ on the cone surface. For the cone+plate, the appropriate solution is positive and vanishes both at $\theta=\Theta$ and $\theta=\pi/2$. The solution in general d requires the use of associate Legendre functions, but simplifies for the generalized wedge geometry (corresponding to $d=2$) described below.[1]

For $d=2$, the problem of a cone coincides with that of a wedge. In higher space dimensions the wedge remains equivalent to the two-dimensional case, as the function $Z(\mathbf{x})$ is independent of the $d-2$ coordinates parallel to the wedge. Thus, the following results for $d=2$ are also applicable to wedges in any d. Equation (**??**) now reduces to $\Psi''+p^2\Psi=0$; which is solved by linear combinations of $\sin(p\theta)$ and $\cos(p\theta)$. The requirement that Ψ is positive and regular, and vanishes on the object(s), yields

$$p_{\rm c}=\frac{\pi}{2(\pi-\Theta)},\quad \text{and}\quad p_{\rm cp}=\frac{2\pi}{\pi-2\Theta}\,. \tag{2.33}$$

Both results go to a finite value as $\Theta\to 0$, reflecting the strong reduction in configurations due to the remnant (barrier) line, and $p\to\infty$ when the boundaries confine the polymer to a vanishing sector. The resulting force amplitude is

$$\mathcal{A}=\frac{2\pi}{\pi-2\Theta}-\frac{\pi}{2(\pi-\Theta)}=\frac{3\pi^2}{2(\pi-\Theta)(\pi-2\Theta)}\,. \tag{2.34}$$

[1] **Exercise:** Perform the corresponding computations in for $d=3$.

3
Role of boundary conditions

3.1 Polymers at the adsorption transition

We considered earlier boundary conditions constraining the field or its gradient. The Dirichlet ($\phi = 0$) and Neumann ($\nabla\phi = 0$) cases are instances of scale-invariant boundary conditions. The mixed (Robin) boundary condition, $\partial_x\phi + \lambda\phi = 0$, on the other hand, does introduce a length scale $\xi = \lambda^{-1}$. Indeed, the solution of the Laplacian operator in $d = 1$ near such a mixed boundary has the form $Z(x) \propto e^{-\lambda x}$.

The exponentially decaying solution actually describes the physical case of random walks (polymers) attracted to the substrate, forming an adsorbed layer of thickness $\xi = 1/\lambda$. As $\lambda \to 0$, the adsorbed layer thickens, and is eventually desorbed. The limiting Neumann boundary condition ($\partial_x\phi = 0$) is thus appropriate for (ideal) polymers right at the desorption transition. Since this boundary condition is again scale invariant, the previous arguments regarding a universal force amplitude are again correct. However, the computation of the force amplitude in terms of γ and p should involve results for the new boundary conditions.

Note, however that for any object with Neumann boundary conditions, $\partial_x\Psi = 0$ implies $\Psi \sim$ constant close to the boundary, and hence $p = 0$ (no depletion). Thus there is no force for any set of objects with such boundaries, and no entropic force is exerted by ideal polymers on any combination of surfaces tuned to be at exactly the desorption transition. There are, however, non-zero forces for mixture of obstacles presenting both Dirichlet and Neumann boundary conditions.

For the wedges considered earlier, there are only two new setups left to calculate, with either the plane or the wedge at the desorption point, as depicted in Fig. **??**.

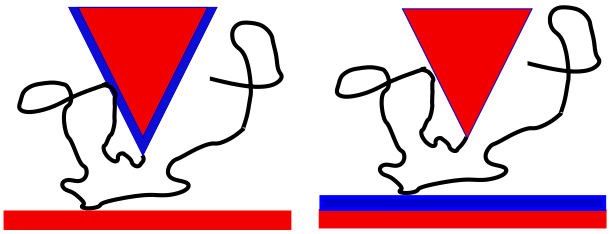

Fig. 3.1 Two variants of cone-plane polymer-mediated setups with mixed boundary conditions: In $d = 3$ we can have an attractive cone and repulsive plane (left), or repulsive cone and attractive plane (right). In $d = 2$ these drawing can be viewed as a wedge approaching a line.

We now need to compute the exponents in the extreme situations, with the wedge touching the line. For the Dirichlet wedge and Neumann line, the condition $\Psi'(\pi/2) = 0$ is satisfied by

$$\Psi(\theta) \propto \sin\left[\frac{(\theta-\Theta)\pi}{(\pi-2\Theta)}\right], \quad \text{with} \quad p'_{\rm cp} = \frac{\pi}{\pi-2\Theta}. \tag{3.1}$$

The force amplitude in this case is given by

$$\mathcal{A}'(\Theta) = p'_{\rm cp} - p_{\rm c} = \frac{\pi^2}{2(\pi-2\Theta)(\pi-\Theta)}. \tag{3.2}$$

In case of the Dirichlet line and Neumann wedge, the conditions $\Psi(\pi/2) = 0$ and $\Psi'(\Theta)$ are satisfied by

$$\Psi(\theta) \propto \cos\left[\frac{2(\theta-\Theta)\pi}{(\pi-2\Theta)}\right], \quad \text{with} \quad p''_{\rm cp} = \frac{2\pi}{\pi-2\Theta}. \tag{3.3}$$

The force amplitude in this case is given by

$$\mathcal{A}''(\Theta) = p''_{\rm cp} - 0 = \frac{2\pi}{(\pi-2\Theta)}. \tag{3.4}$$

3.2 Repulsive quantum Casimir force

Having noted the importance of mixed boundary conditions in case of polymers, let us reexamine the effect of such mixing in case of the quantum Casimir force. Consider a one-dimensional interval supporting a quantum field subject to boundary conditions $\phi(0) = 0$ and $\partial_x\phi(H) = 0$. The resulting modes $\sin(q_n x)$ have wavenumbers $q_n = (2n-1)\pi/(2H)$ for $n = 1, 2, \cdots$.

Modifying the earlier computation, the ground state energy in this case is obtained as

$$E_0(H) = \sum_{n=1} \frac{\hbar\omega_n}{2} = \frac{\hbar c}{2}\frac{\pi}{H}\sum_{n=1}\left(n-\frac{1}{2}\right) = \frac{\hbar c}{2}\frac{\pi}{H}\left(\sum_{n=1} n - \frac{1}{2}\sum_{n=1} 1\right) . \tag{3.5}$$

Following zeta-function regularization, the first sum becomes -1/12, and the second sum -1/2, resulting in

$$E_0(H) = +\frac{\hbar c}{H}\frac{\pi}{12} \qquad \text{and} \qquad F(H) = -\frac{dE_0}{dH} = +\frac{\hbar c}{H^2}\frac{\pi}{12} . \tag{3.6}$$

Note that the Casimir force is now positive in this mixed geometry.

A similar computation shows that mixed boundary conditions for the quantized scalar field in three dimensions lead to a repulsive Casimir pressure of [1]

$$\beta P = -\frac{\partial E_0(H)}{A\partial H} = +\frac{\hbar c}{H^4}\cdot\frac{7\pi^2}{60}. \tag{3.7}$$

[1] **Exercise:** Prove the quoted result for the quantum Casimir force in $d = 3$ with mixed boundary conditions.

3.3 Stability and Earnshaw's theorem

A question that has considerable interest is whether the Casimir force can, for some geometry, be repulsive.The practical importance of such a finding, is a way to avoid stiction, the sticking together of components of a microelectromechanical machine due to the attractive force.Repulsion can indeed occur between if the space between two dissimilar plates is occupied by a medium (e.g. fluid) of dielectric constant intermediate between the two plates. This is a situation that mimics the case of mixed boundary conditions discussed above. However, it is impractical to immerse components of a micro-machine, composed of distinct dielectrics inside a fluid. The exciting possibility is to achieve such a repulsion across vacuum, by manipulating shape or electromagnetic response of the bounding plates.

The possibility of such repulsion was partly motivated by a calculation by Boyerwho found the Casimir energy of an infinitely thin perfectly conducting spherical shell to be positive. The square in two dimensions, and the cube in three dimensions, also have a positive Casimir energy in this sense. It is of course essential to establish the presence of repulsion in a physical context in which all other material forces (cohesion, surface tension, etc.) are under control. The piston geometryin which a partition slides inside a box provides such an example, and is related to some geometries where a repulsive force is claimed. We showed,however, that the partition is unstable and attracted to the closest boundary.

The example of the piston suggests that the pertinent question is not if the partition is attracted by one or the other base of the piston, but if there is a point of *stable equilibrium* in between. The absence of such would bode ill for avoiding stictionor achieving levitation.For classical electrostatics, this is precisely addressed by *Earnshaw's theorem*: The potential ϕ acting on a set of charges satisfies Laplace's equation, $\nabla^2\phi = 0$, in free space. This immediately rules out a stable equilibrium position, which say for a positive charge would require $\nabla^2\phi > 0$. Is there a version of this theorem for *fluctuation-induced interactions?*

At least for some classical situations, the answer is positive: Consider a collection of non-overlapping enclosures ('bags'), each containing a fluctuating set of charges that can move around, appear and disappear in pairs while maintaining overall charge neutrality in each bag. This is closely related to ionic mixtures of charged macroions and compensating counterions in a solvent; a system much studied within soft-matter and biological contexts. An effective FIF between the bags results from averaging over configurations of the mobile charges in solution. The forces can be obtained from variations of the free energy

$$-\beta\mathcal{F}(\{\mathbf{R}_i\}) = \ln\left[\int \prod_\alpha d\mathbf{r}_\alpha \exp\left(-\beta\phi[\mathbf{R}_i, \mathbf{r}_\alpha]\right)\right], \tag{3.8}$$

where $\{\mathbf{R}_i\}$ are the (constrained) coordinates of the bags, $\{\mathbf{r}_\alpha\}$ are the positions of the mobile charges, while $\phi[\mathbf{R}_i, \mathbf{r}_\alpha]$ is the total electrostatic energy. Note that in this classical context, the fluctuations are entirely of thermal origin, $\beta = 1/(k_B T)$, and quantum mechanics plays no role. The stability of a 'bag' in this effective potential can now be checked by considering $\nabla_i^2\mathcal{F}$, where the gradients are with respect to the

position $\mathbf{R}_i$ of the bag. Standard manipulations of the above formula yield

$$\nabla_i^2 \mathcal{F}(\{\mathbf{R}_i\}) = \langle \nabla_i^2 \phi(\{\mathbf{R}_i\})\rangle - \beta \left(\langle |\nabla_i \phi|^2 \rangle - |\langle \nabla_i \phi \rangle|^2 \right) \leq 0. \tag{3.9}$$

Note that the first term is zero because of Laplace's equation– the origin of the standard Earnshaw's theorem. The second term is negative, as it is (minus) the variance of a fluctuating force. Fluctuations thus tend to destabilize, and the containers cannot find a position of stable equilibrium.

For the quantum Casimir force, the container in the above picture are replaced by neutral objects (metals or dielectrics), and the quantized EM field takes the place of the thermally fluctuating charges. Ideas similar to the above calculations were used by us to demonstrate an analog of such an Earnshaw constraint for material composed entirely of dielectrics of arbitrary shape, as long as their response to the electromagnetic field can be captured by a classical dielectric function $\epsilon(\mathbf{x}, \omega)$, which can in principle vary across space and frequency (subject to usual stability criteria).